

# Actionable and diverse counterfactual explanations incorporating domain knowledge and causal constraints

Szymon Bobek `szymon.bobek@uj.edu.pl`<sup>1</sup>, Łukasz Bałec  
`l.bałec@cyberfolks.pl`<sup>2,3</sup>, and Grzegorz J. Nalepa  
`grzegorz.j.nalepa@uj.edu.pl`<sup>1</sup>

<sup>1</sup>Faculty of Physics, Astronomy and Applied Computer Science, Institute  
of Applied Computer Science, Jagiellonian Human-Centered AI Lab

<sup>2</sup>`cyber_Folks`<sup>TM</sup>, Krakow, Poland

<sup>3</sup>FreshMail Sp. z o.o., Krakow, Poland

December 1, 2025

## Abstract

Counterfactual explanations enhance the actionable interpretability of machine learning models by identifying the minimal changes required to achieve a desired outcome of the model. However, existing methods often ignore the complex dependencies in real-world datasets, leading to unrealistic or impractical modifications. Motivated by cybersecurity applications in the email marketing domain, we propose a method for generating Diverse, Actionable, and kNoledge-Constrained Explanations (DANCE), which incorporates feature dependencies and causal constraints to ensure plausibility and real-world feasibility of counterfactuals. Our method learns linear and non-linear constraints from data or integrates expert-provided dependency graphs, ensuring counterfactuals are plausible and actionable. By maintaining consistency with feature relationships, the method produces explanations that align with real-world constraints. Additionally, it balances plausibility, diversity, and sparsity, effectively addressing key limitations in existing algorithms. The work is developed based on a real-life case study with Freshmail, the largest email marketing company in Poland and supported by a joint R&D project *Sendguard*. Furthermore, we provide an extensive evaluation using 140 public datasets, which highlights its ability to generate meaningful, domain-relevant counterfactuals that outperform other existing approaches

based on widely used metrics. The source code for reproduction of the results can be found in a GitHub repository we provide.

## 1 Introduction

Explainable Artificial Intelligence (XAI) has gained substantial momentum in recent years, attracting attention from both researchers and various business sectors, including healthcare, heavy industry, and legal firms. A multitude of XAI methods were developed, each addressing different facets of explaining AI system decisions. The type of explanation depends primarily on the objective that the explanation should achieve (model improvement, model debugging, bias detection, etc.) and the target audience to which the explanation is directed (data scientist, domain expert, end user) [6].

Counterfactual (CF) and contrastive explanations are often the most valued by stakeholders such as end-users and domain experts [9, 24] because they give explicit examples of which features play the most influential role in AI models' decisions and how their values should be changed in order to modify the overall AI system output. However, CF explanations that conflict with established domain knowledge or common sense are particularly problematic, as they fail to provide actionable insights and reduce trust in the AI system. For example, a CF explanation suggesting that reducing the risk of diabetes involves altering parameters such as sex, age, and pregnancy status would be deemed impractical and irrelevant, given the well-established medical understanding of diabetes management and common sense. Despite this, only a minority of existing methods for generating CFs consider plausibility, and none approach the problem from a comprehensive perspective that accounts for other factors such as proximity, diversity, and sparsity. This issue has become one of the emerging challenges in the XAI area, not only limited to counterfactual explanations [11], but most often in practical implementation of XAI methods to different business cases.

Our work is on the one hand directly rooted in the very active area of basic CF research in XAI (see Section 2), yet on the other hand is motivated by practical challenges in a specific domain, which is cybersecurity in online marketing. In this case the ability to generate domain-informed, plausible counterfactuals stands to substantially enhance the relevance and quality of email campaigns, newsletters and communication with customers. In this context, a counterfactual should provide actionable insights, suggesting specific alterations to a campaign (e.g., changing the subject line length, adjusting the send time, or refining the image-to-text ratio) to improve its perceived quality. However, the recommended modifications that do not align with industry best practices, contradict known audience prefer-

ences, or violate brand guidelines are unlikely to be adopted by practitioners, thus limiting their practical utility. Our work stems from a collaboration with Freshmail<sup>1</sup>, the largest email marketing company in Poland, and their real-life business case that gave motivation for our research is described in Section 3.

To address the above mentioned challenges, we propose the DANCE method (*Diverse, Actionable, and kNowledge-Constrained Explanations*) which learns linear and nonlinear constraints from data or integrates expert-provided dependency graphs, ensuring counterfactuals are plausible and actionable. Furthermore, it maintains consistency with feature relationships, and thus produces explanations that align with real-world constraints. Additionally, it balances important qualities including plausibility, diversity, and sparsity, effectively addressing key limitations in existing state-of-the-art algorithms. The systematic description of the method we propose is provided in Section 4.

We provide an extensive evaluation of the method. We performed quantitative analyses, as we tested our method on over 140 benchmark datasets from OpenML [5], comparing it with other methods, and demonstrated that it consistently achieves the highest scores across all approaches in Section 5. Furthermore, we provided qualitative analyses on a real dataset from Freshmail’s business case in Section 6.

Let us now move to the discussion of the state-of-the-art solutions in the field of counterfactual generation and highlight the research gap that our work aims to address.

## 2 Related works

The XAI research area has experienced a blooming period over the recent years, which was driven both by the researchers who noticed the urgency of providing more control over the AI systems operation [29], as well as legal authorities through the AI Act in UE [15], and DARPA challenge [12] in the USA. The full spectrum of XAI methods is vast and has been extensively covered by several surveys [17, 1, 4], to which we refer readers for a comprehensive overview of the field. In this work, we focus specifically on counterfactual explanations, a distinct subfield within XAI that provides example-based explanations [31].

In this type of XAI method, the explanations are presented to the user as examples of specific instances, which may be real or artificially generated. For tabular data, the explanation takes the form of a row of feature values; in the case of image data, it is an image; and for text data, it is a text snippet, etc. Counterfactual explanations further ensure that the instance belongs to a contrasting class (potentially

---

<sup>1</sup><http://freshmail.pl>

defined by the user) relative to the instance being explained.

Other methods for example-based explanations include adversarial examples [4], prototypes and critiques [21], and explanations based on prototypical parts [10], among others. What distinguishes counterfactual explanations from these types is that counterfactuals are expected to meet certain additional properties. The most common properties are correctness, diversity, sparsity, proximity, and plausibility [17]. However, no existing methods optimize for all these properties simultaneously; instead, they typically focus on just a subset.

Furthermore, very few methods prioritize the plausibility of counterfactuals. Those that do often use simple range-based constraints, which limit the ability to capture more complex relational constraints - this is precisely where our work focuses. Additionally, these methods typically do not permit expert interaction with the constraints, thereby disabling domain-knowledge-based constraints and relying solely on density-based and data-driven constraints to model plausibility. In the following paragraphs, we provide a more in-depth analysis of existing methods with respect to correctness, diversity, sparsity, proximity, and plausibility criteria. Our focus is on methods that address plausibility in some form or are considered significant milestones in the counterfactual generation landscape. A comparative summary of these methods is provided in Table 1. For a comprehensive review of all methods in the field, we refer the reader to [17].

One of the earliest counterfactual generation methods was Wachter [33]. It used a simple approach that minimized a loss function composed of two terms: one for the proximity of the counterfactual and the other for its correctness. This basic loss function was optimized using the Simplex algorithm. The Wachter algorithm is often regarded as a baseline for other methods, as it was both the first and one of the most straightforward approaches to counterfactual generation.

DCE [28] followed a similar idea as introduced in WACH, but optimizing a custom cost function that accounted for sparsity and proximity, but added component responsible for keeping the counterfactual coherent. The authors defined coherence as consistency with the underlying data structure, which was limited to ensuring that the counterfactual generation method does not set all one-hot-encoded features to either  $0$  or  $1$ . In this sense, we can consider this approach as a minimal plausibility constraint. DCE was designed only to work with linear models.

One of the most well-known methods in the area of CF is called Diverse Counterfactual Explanations (DICE) [25]. It further extends the ideas of Wachter and DCE by including additional terms in the loss function to ensure the broader spectrum of CF properties. It was designed to handle diversity, sparsity, and proximity of counterfactual with a custom loss function that integrated all of the three criteria in a form of losses and optimized with different forms of search algorithms such as

genetic algorithms, random search, gradient optimization. It utilized hinge loss to decide on the correctness of the counterfactual. DICE does not directly account for plausibility in the objective function but allows for predefined ranges of feature values, which can help prevent implausible counterfactuals, such as values outside the possible scale or basic monotonicity constraints (e.g. age cannot decrease). A similar approach to handling implausible feature values was proposed in MACE [20] and CFNOW [13]. None of the aforementioned methods consider complex cases, where the constraints are conditional, or in some kind of relation (e.g. linear) with respect to each other.

Another group of methods approaches plausibility through representation learning. This includes algorithms such as CEM [14], EBCF [23], and CEGP [32], or FRACE [36]. These methods rely on autoencoders to ensure that the reconstruction loss of a newly generated sample (counterfactual candidate) is minimal, confirming that it is plausible—that is, that it belongs to the representation learned by the autoencoder during training.

Finally, the last group of methods ensures the plausibility of newly generated samples by positioning them in areas of high-density points or aligning them with the underlying data distribution. This group can be further divided into endogenous explainers, which provide explanations by selecting existing samples from the given dataset (such as LUX [7], LORE [18]), and exogenous explainers, which generate artificial samples such as DACE [19], OCEAN [27], or PPCF [35].

The motivation for our work, which stemmed from the visible gap in the landscape of state-of-the-art counterfactual explainers, was additionally backed by the practical needs. A detailed description of the business motivation is given in the following section.

### **3 Motivation grounded in practical use case from cybersecurity in email marketing**

In the rapidly evolving digital landscape, Communication Platform as a Service (CPaaS) providers have gained critical importance by enabling businesses to efficiently engage with their audiences through various communication channels. Among these channels, email marketing remains a fundamental tool for customer outreach, brand awareness, and relationship building. Modern CPaaS solutions offer comprehensive platforms for creating, managing, and distributing large-scale email campaigns. However, ensuring that these messages are both welcomed by recipients and meet stringent quality standards poses a significant challenge. The delicate balance between delivering valuable, personalized promotions and avoiding unwanted or irrelevant content – colloquially known as spam – lies at the core

of the email marketing domain.

Furthermore, there is a growing trend in cybersecurity, to fight misinformation in all possible channels. Thus, carefully engineering spam messages that could be injected into a viable marketing campaign can cause an important security threat. Although in the work described in this paper we consider content quality on a general level, and do not address cybersecurity directly, the technology we developed within the *Sendguard* project with Freshmail is in fact security-oriented [16]. The project co-financed by the Polish National Centre for Research and Development (NCBiR) between 2020-2023 aimed at developing a number of AI-based techniques to strengthen the security of company mail-servers by protecting them from sending spam or phishing messages.

Freshmail offers its customers a diverse platform for email marketing. It is most commonly used with so-called marketing campaigns that their customers design with their marketers. A campaign is first designed around a given topic, with a number of factors regarding both content and its form identified and configured. Furthermore, possible target groups of campaign recipients are identified. Using such a configuration, and additional schedules based on expert knowledge (e.g. when specific target groups tend to read their emails), large batches (tens or even hundreds of thousands) of email messages are sent. Quality of messages is important not only from marketing point of view, but also security. Should there be an increased level of low quality messages sent, the company servers could be put on blacklists by backbone Internet providers and effectively blocked from operation.

In this work here, to quantify undesirability of email messages, we adopted an engagement-centric metric: an extremely low email open rate (e.g., less than 2%) suggests that recipients do not find value in the content. While straightforward in principle, this approach surfaced deeper issues. The open rate alone could not fully explain the complex interactions among countless features that influence campaign performance. Factors such as subject line specificity, visual composition, send time, and audience segmentation all interweave to determine how a campaign is received.

This multifaceted nature of campaign data, enriched by detailed server logs, event records, and behavioral analytics, made classification and prediction profoundly challenging. Consequently, understanding why a model identified a campaign as undesirable was nearly as difficult as classifying the campaign itself. This realization underscored the necessity for the use of XAI methods. Introducing XAI techniques enabled us to decipher the reasoning behind model predictions, illuminating which features or interactions influenced the classification of a campaign as spam-like. Such a transparency is instrumental in guiding both model refinement and practical improvements to the campaigns themselves. Instead of simply labeling a campaign as undesirable, explanations, such as counterfactuals, guide

marketers in transforming an ineffective campaign into one that engages and resonates with recipients.

While counterfactual explanations hold significant promise, existing generation methods are often limited by restrictive assumptions. Standard approaches frequently overlook the complex joint distributions and dependencies present in real-world datasets. In real world scenarios, unrealistic or impractical changes proposed by counterfactuals limit their adoption and business value. From the company perspective, the ability to generate domain-informed, plausible consistent counterfactuals stands to substantially enhance the relevance and quality of email marketing campaigns. Having this requirement as a practically grounded motivation, our research highlights a path forward for integrating complex data-driven models with domain expertise to produce results that are not only correct in theory but also valuable in practice.

In the following sections, we detail the algorithmic foundations of our approach, followed by empirical evaluations validating its benefits, and the broader implications for the future of AI-driven marketing communications and its security.

## 4 Method description

### 4.1 Background

We introduce a novel method –DANCE –which stands for Plausible Constrained Counterfactuals. It allows us to learn the structure and magnitude of dependencies between features used by the blackbox model in the form of linear or nonlinear constraints on the feature values. This structure is then used to generate counterfactuals consistent with it, hence plausible and therefore more actionable. Alternatively, the structure and/or specific constraint values can be provided in advance by an expert if they are known *a priori*.

We are focusing on two types of relation between features: a linear relation and possibly nonlinear conditional relations. As the CF by definition is an instance that is produced by altering features values of the original instance, the relations ensure that modifications are consistent with given relations. We employ a custom cost function to ensure not only plausibility, but also diversity and sparsity of explanations given in equation below and employed Tree-structured Parzen Estimator optimization algorithm to minimize it [34]. Figure 1 shows the cases that our method handles.

The linear relation between features prevent the method from altering only one feature value without changing the value of another one. The relation can be provided in a form of directed acyclic graph, where nodes represent variables and edges contain information about the linear relationship between them. This can

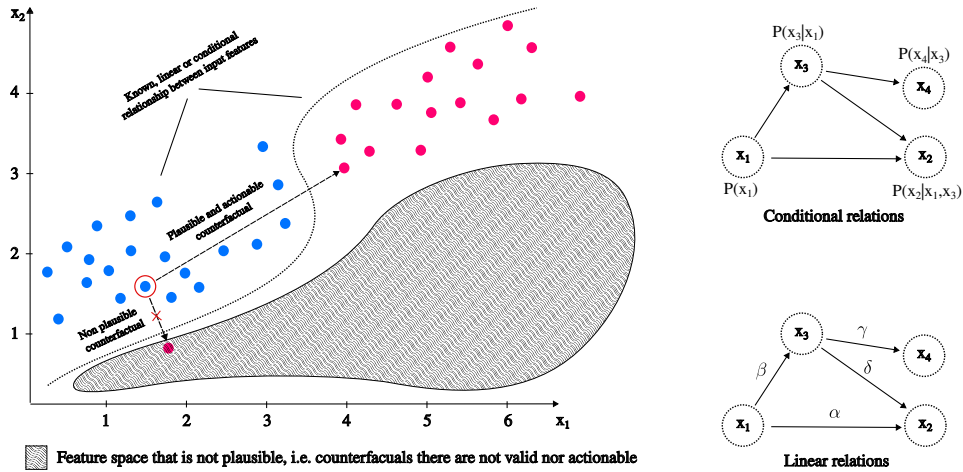


Figure 1: Example of a relation between input variables that will not be captured by existing methods, but can be modeled with linear or conditional constraints and our approach.

be used to describe linear relationships such as *"Increasing the ambient pressure, increases the temperature of boiling of a liquid"*.

Conditional dependencies allow one to model more complex constraints that are non-linear, e.g. mark "forbidden" feature space areas. Similarly to the previous type of constrains, this type is also defined by the directed acyclic graph, however, the nodes contain conditional probability distribution of feature value given the feature values of nodes from incoming edges. This in fact can be modeled in the form of a Bayesian network and can handle relationships that are more complex than simple linear constraints such as the aforementioned forbidden areas in the feature space: *"Given the person is a man, the probability of him being pregnant equals 0"*.

The core of our approach was to design and optimize a loss function in a way that will evenly value different properties of final set of counterfactuals such as fidelity, proximity, sparsity, plausibility, and diversity. For the design of the loss function, we build on the concepts introduced by Wachter and DICE, integrating different properties as separate components of the function, as shown in Equation (1).

$$L = \underbrace{\max \left[ 0, \max_{c \neq d} (\hat{P}_{i,c} - \hat{P}_{i,d}) \right]}_{\text{Maximum of zero and difference between maximum probability of desired class } d \text{ versus other classes.}} + \underbrace{\lambda \cdot (\omega_d \cdot L_d + \omega_n \cdot L_n + \omega_s \cdot L_s + \omega_p \cdot L_p)}_{\text{Diversity, Proximity, Sparsity and Plausibility losses respectively with their weights. The } \lambda \text{ parameter is global weight for the term.}} \quad (1)$$

The first term ensures the correctness of the counterfactual by enforcing that the predicted probability of the desired class exceeds that of all other classes. It is formulated as a hinge loss that becomes zero once this condition is satisfied, guaranteeing the intended classification change. In Figure 1, this corresponds to moving the query point across the decision boundary. However, simply crossing the boundary is not enough to make a counterfactual useful. The second term determines where the counterfactual is placed, ensuring it does not end up in an arbitrary region but in a part of the feature space that makes it actionable. This is achieved through a weighted combination of property-specific objectives—plausibility, proximity, sparsity, and diversity—that must be carefully balanced. For example, a minimal change that violates domain constraints may technically achieve the desired prediction but remains unrealistic and therefore not actionable. Figure 1 illustrates why plausibility is critical: counterfactuals should respect both conditional dependencies (e.g.,  $P(x_2 | x_1, x_3)$  and  $P(x_4 | x_3)$ ) and linear relationships among features. Ignoring these relationships can lead to invalid suggestions, such as feature combinations that cannot occur in practice. By jointly optimizing these properties, the approach ensures that counterfactuals are not only effective in altering predictions but also realistic, interpretable, and suitable for decision-making. A key challenge in this approach is ensuring that each component is balanced in magnitude, preventing any one term from dominating the others. To address this, we propose defining each component so that it is scaled between 0 and 1, allowing for more intuitive hyperparameter tuning and facilitating a more reliable search for optimal values.

In the following sections, we describe in-depth the design of particular loss components and the process of search for optimal solution.

## 4.2 Plausibility

The plausibility in our approach is defined as a consistency of a newly generated sample (counterfactual candidate) with the predefined relationships between feature values. This relationship can be given a priori by the expert (in which case it may also be considered causal) or can be discovered automatically from the data. In the case of automatic graph discovery, we use the DirectLiNGAM method [30]

for linear relationship graph discovery. For conditional probability graph learning we use again DirectLiNGAM, or NOTEARS [37] for structure learning and estimate probability distribution with Bayesian parameter estimation. In both cases, the relationships are represented in our approach as a directed acyclic graph (DAG) as presented in Figure 2. From a practical point of view, in the implementation of our method, the graph is represented as an adjacency matrix. In the following paragraphs, these two approaches are described in more detail.

**Discovery of relationships with graph** DirectLiNGAM [30] assumes that the data is generated by a linear non-Gaussian acyclic model (LiNGAM), defined as:

$$\mathbf{x} = \mathbf{B}\mathbf{x} + \mathbf{e} \quad (2)$$

where  $\mathbf{x} \in \mathbb{R}^d$  is the vector of observed variables,  $\mathbf{B} \in \mathbb{R}^{d \times d}$  is a strictly lower triangular matrix encoding the causal structure, and  $\mathbf{e} \in \mathbb{R}^d$  is a vector of independent, non-Gaussian noise terms. The method identifies causal ordering by iteratively detecting exogenous variables - those independent of regression residuals. For each variable  $x_j$ , residuals  $r_i^{(j)}$  are computed by regressing other variables  $x_i$  on  $x_j$ , and independence is tested:

$$x_j \perp r_i^{(j)} \quad \forall i \neq j \quad (3)$$

The intuition behind this is that if  $x_j$  is truly exogenous, then any dependence of  $x_i$  on  $x_j$  must be due to  $x_j$ 's influence on  $x_i$ , not the reverse. This is because if we regress  $x_i$  on  $x_j$ , the residual  $r_i^{(j)}$  captures the part of  $x_i$  that is not explained by  $x_j$ .

If  $x_j$  is exogenous, then it should be statistically independent of the residuals  $r_i^{(j)}$ , because  $x_j$  is not influenced by any other variable and the residuals represent influences from other variables or noise, which are independent of  $x_j$ .

Therefore, if the variable is exogenous, i.e.  $x_j = \mathbf{e}_j$  it becomes the parent node in the graph. Once the ordering is established, the matrix  $\mathbf{B}$  is estimated via least squares regression. The  $\mathbf{B}$  represent the linear relationship graph. For instance, in Figure 2 the relationship for well known Wine dataset [2] was presented which was calculated with the described method. As discussed earlier, the  $\mathbf{B}$  is strictly lower triangular, therefore no cycles are observed in the graph, and the non-zero elements at the intersection of rows and columns indicate the weight of the edge (the relation between features) depicted in the graph.

**Conditional Probability Distribution Estimation** Once the causal structure is obtained using DirectLiNGAM or NOTEARS, we additionally allow to estimate

the conditional probability distributions (CPDs) for each node in the resulting directed acyclic graph (DAG). If the observed variables are continuous, we first discretize them into a finite number of bins, transforming the data into categorical form suitable for discrete probabilistic modeling.

We employ the Bayesian parameter estimation, which provides tools for learning CPDs from data given a fixed DAG structure. For each variable  $X_i$ , the conditional probability distribution  $P(X_i | \text{Pa}(X_i))$  is estimated using maximum likelihood estimation (MLE) or Bayesian estimation, where  $\text{Pa}(X_i)$  denotes the set of parent variables of  $X_i$  in the learned structure.

Each CPD is represented as a conditional probability table that specifies the probability of each discrete state  $X_i = x_i$  given all possible configurations of its parent states  $\text{Pa}(X_i) = \mathbf{x}_{\text{pa}}$ :

$$P(X_i = x_i | \text{Pa}(X_i) = \mathbf{x}_{\text{pa}}) = \frac{N(X_i = x_i, \text{Pa}(X_i) = \mathbf{x}_{\text{pa}})}{N(\text{Pa}(X_i) = \mathbf{x}_{\text{pa}})},$$

where  $N(\cdot)$  denotes the empirical count in the discretized dataset.

The resulting set of CPDs defines a fully parameterized Bayesian network consistent with the discovered causal structure, enabling probabilistic inference and sampling over the joint distribution of all variables. Compared to using the linear coefficients from DirectLiNGAM, this discretized CPD approach has the advantage of capturing potentially nonlinear or non-monotonic relationships between each variable and its parents, since each parent configuration is associated with an empirically estimated probability distribution rather than a fixed linear effect.

**Plausibility loss estimation** Having the relationship graph, we now are able to test each counterfactual candidate against its consistency with it. In order to do that, we pass the sample through the graph in an order obtained from topological sorting and in each node we calculate the difference between the actual sample value and the value obtained by sum of values of its parent nodes multiplied by the weights on the edges. The final error is additionally averaged over the number of nodes in the network to ensure that the result is approximately within 0 and 1 range. The formulae for calculation of the plausibility loss is given in Equation (4). The loss  $L_p$  is calculated as the mean squared error (MSE) over all nodes in the graph  $G = (V, E)$ , where  $V$  represents the set of features, and  $E$  represents the edges (linear relationships) between the features or their conditional probability dependencies represented by weights  $w$ .

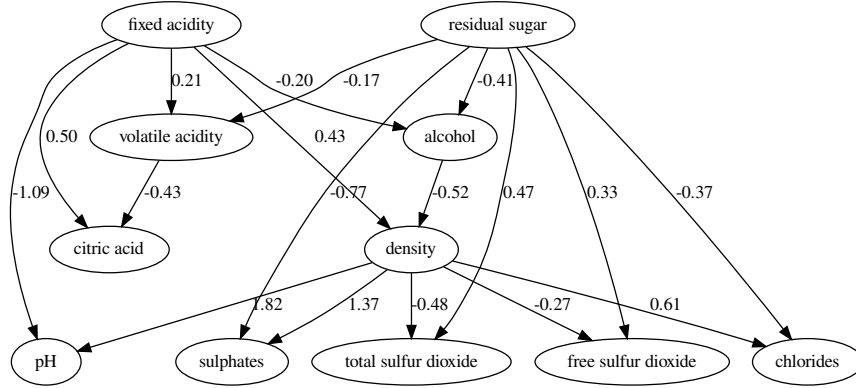


Figure 2: Relationship graph for a Wine dataset. The edges represent the magnitude in which change in the parent node values impact the children node values. For instance increase in residual sugar decreases the alcohol in the wine and the counterfactual that not preserve this constrain is considered implausible and not actionable.

$$L_p(\text{cf}, V, E) = \frac{1}{|V|} \sum_{i=1}^{|V|} (\text{cf}_i - v_i)^2 \quad (4)$$

$$v_i = \sum_{p \in \text{Parents}(v_i)} w_{p \rightarrow i} \cdot x_p$$

In the Equation (4), the  $\text{Parents}(v_i)$  denotes the set of parent nodes of  $v_i$  in the graph, which reflects the dependent features. The  $w_{p \rightarrow i}$  is the weight associated with the edge from parent  $p$  to node  $v_i$  and  $x_p$  is the feature value of the parent node  $p$ .

### 4.3 Proximity

The proximity is one of the fundamental property for a counterfactual that ensures that the explanation will be similar to the instance fro which is is generated. For that, we use the weighted cosine similarity on normalized instances. This allows us to calculate the similarity as a weighted dot product of two vectors as shown in Equation (5).

$$L_d(\text{cf}, x) = \frac{1}{M} \sum_{i=1}^M \omega_i \cdot \text{cf}_i \cdot x_i \quad (5)$$

The usage of cosine similarity instead of euclidean distance makes the computation more efficient and less prone to curse of dimensionality [3].

#### 4.4 Sparsity

The sparsity measures how drastic is the modification of an original instance is in order to transform it into counterfactual, which by the definition is the *minimal* change in original feature. In practice, this is reduced to the number of features that values' were altered in CF compared to original instance, as shown in Equation 6.

$$L_s(\text{cf}, x) = \frac{1}{M} \sum_{i=1}^M \mathbb{I}(\text{cf}_i - x_i) \neq 0 \quad (6)$$

Note, that the function is non-convex, hence it cannot be included in the loss function if the optimization is gradient-based. However, but we use optimization method that works with non-convex functions and allows us to include it in the total loss.

#### 4.5 Diversity

In case of diversity, we used determinantal point process to estimate the variety of counterfactuals generated in a final set, similarly to [25]. This allowed us to keep the measure bounded by 1 which was one of our objectives in the loss function design.

The equation for that is given in Equation 7. Note that the diversity is a property of counterfactuals only, regardless of the instance for which the CFs were generated.

$$L_d(\text{cfs}) = \det(K) \quad (7)$$

Where,  $K$  is a distance matrix between counterfactuals, defined below. The  $\delta$  is a Kronecker delta that equals 0 for all  $i$  and  $j$  except the case when  $i = j$ , when it is equal to 1. In practise, this adds small random noise to diagonal elements to avoid ill-defined determinants.

$$K_{i,j} = \frac{1}{1 + \|\text{cf}^{(i)} - \text{cf}^{(j)}\|_2 + \epsilon \cdot \delta_{ij}}$$

All of the components  $L_d, L_n, L_s, L_p$  described before are finally added to the global loss function presented in Equation 1 and optimized with an approach presented in following section.

## 4.6 Counterfactual search

The process of search for counterfactuals can be divided into three stages that are executed in the following order. The compact representation of this process is also presented in Algorithm 1.

1. In the first stage, the relationship graph is created. It can be either generated automatically in a data-driven manner or provided explicitly by the expert. If the full graph is not known, only partial relationships can be defined.
2. In the second stage, data generation is performed to create a pool of counterfactual candidates. The initial set of candidates is generated by sampling from the provided dataset, or, if unavailable, by generative sampling from the relationship graph. In the case of additive and linear models, data can also be generated using information about feature contributions similar to [28] and [19].
3. Finally, the loss function is optimized using a Tree-Structured Parzen Estimator [34] which is a kind of Bayesian optimization approach that allows for tree structure search spaces (i.e. spaces with possible conditional parameters).

One of the most important parts of the method is the relationship graph that captures causal dependencies between variables and represents linear or probabilistic relationships between features' values. Figure 2 presents a sample graph trained on the well-known Wine dataset [2] which was selected solely for illustrative purposes due to its simplicity and widespread familiarity, which help to clearly demonstrate the underlying concepts. The structure and coefficients on the edges were learned using DirecLinGAM approach. As mentioned previously, the graph paragraph can be obtained from experts (fully or only partially) or can be learned automatically from the data. If the graph is provided by the expert, it does not have to be complete, as the method automatically finds missing relationships from the data. The graph is used in the plausibility loss component to ensure that the counterfactual is aligned with it and does not contain feature values that are not consistent with the background knowledge.

Additionally to relationship graph, we can narrow the search space with range-based constraints, such that prevent certain variables from taking certain values

---

**Algorithm 1** DANCE Counterfactual search algorithm

---

**Input:** Blackbox Model  $M$ ; Training dataset  $X$ ; Relationship graph  $G$ ; Desired number of counterfactuals  $N$ ; Weights  $\omega$  for the loss function from Equation (1); Desired class  $d$

**Output:** List  $CF$  of  $N$  counterfactual examples

Initialize result set  $CF \leftarrow \emptyset$ ;

**if**  $G = \emptyset$  **then**

    Train  $G$  with  $X$  and LinGam, or Bayesian parameter estimation

**end if**

**for**  $i \in 1, 2, \dots, N$  **do**

    Create initial counterfactual candidates  $X'$

$X' \leftarrow$  samples from  $X$  and generated with  $G$

**if**  $M$  is additive or linear **then**

$X' \leftarrow$  samples generated from  $M$

**end if**

    Find counterfactual  $cf_i \leftarrow \arg \min_{cf_i} L(M, cf_i, CF, G, X', d, \omega)$

    Add  $cf_i$  to the result set  $CF \leftarrow \{cf_i\} \cup CF$

**end for**

**Return:** List of plausible, diverse, and sparse counterfactuals  $CF$

---

(i.e. values from outside of the domain, or forbidden values (e.g. age of a person lower than actual). Such constraints also allow us to mask features that should not be modified at all by the algorithm.

Our method ensures diversity among counterfactuals, allowing the desired number of counterfactuals to be specified as output. Counterfactuals are generated sequentially: in the first iteration, the best counterfactual is identified, and in subsequent iterations, additional diverse counterfactuals are sought.

## 5 Quantitative evaluation

We compared our method with the selected methods from the state-of-the-art. We focused only on the methods that are model-agnostic and have existing implementation. Additionally, we performed an ablation study, where we excluded the plausibility component from our method to observe what impact it has on the remaining criteria such as diversity, sparsity, etc. We tested our method on 140 datasets from OpenML<sup>2</sup> repository. Detailed results from the evaluation of specific properties are

---

<sup>2</sup>See: <https://www.openml.org/>.

provided in the appendices. We used Explainable Boosting Machine (EBM) [22] model as a classification model. The source code for reproduction of the results can be found in our GitHub repository<sup>3</sup>. The precomputed metrics for all of the methods and dataset can be found in the supplementary materials.

## 5.1 Analysis of the results

A summary of these results is shown in Figure 3. The plot presents the scores obtained by each method across 140 datasets. The score is calculated as the area under a spider plot (AUS) in a form of sum areas of triangles defined by the center of the plot and neighborhood vertices. Each vertex representing the  $\frac{1}{R_i}$  of a method, where  $R_i$  is the average ranking obtained from Friedman post-hoc statistical tests for the  $i$ -th property of a given method. The formulas for this combined metric is given in Equation (8). The closer a method’s score is to the maximum possible area defined as  $\frac{NM^2}{2} \sin\left(\frac{2\pi}{N}\right)$ , the better its overall performance. The  $M$  represents the total number of methods tested.

$$AUS = \frac{1}{2} \sin\left(\frac{2\pi}{N}\right) \sum_{i=1}^N \frac{1}{R_i R_{i+1}} \quad (8)$$

This evaluation method is adopted from [7], where the authors use it to illustrate multi-criteria evaluation results in scenarios where there is a known trade-off between the metrics. The area can be affected by the order of vertices, hence it is recommended to put metrics that there is known trade-off between (e.g. precision and recall) next to each other. In the plot, we included *probability* metric showing how confident the model predictions were for a given counterfactual. In our case, all metrics are treated equally as the trade-off exists between all of them.

Additionally, we tested the statistical significance of the differences of our method compared to the rest. We have conducted Friedman post-hoc test followed by Nemenyi test and have proven that our method is significantly better than others in causality and sparsity and probability metrics. In the remaining metrics, it also achieved top scores, but the differences were not statistically significant. The only metric that our method was not the best was diversity, where it lost to Wachter, DICE and LORE. This is particularly remarkable because Wachter and LORE does not inherently optimize counterfactuals for diversity. Instead, we simulated this by running Wachter and LORE multiple times and collecting results from each run. As a result, the observed diversity was primarily due to the stochastic nature of counterfactual generation implemented within these methods. The critical distance plots and statistical analysis of the tests are provided in A.

<sup>3</sup>See: <https://github.com/sbobek/xaibench>.

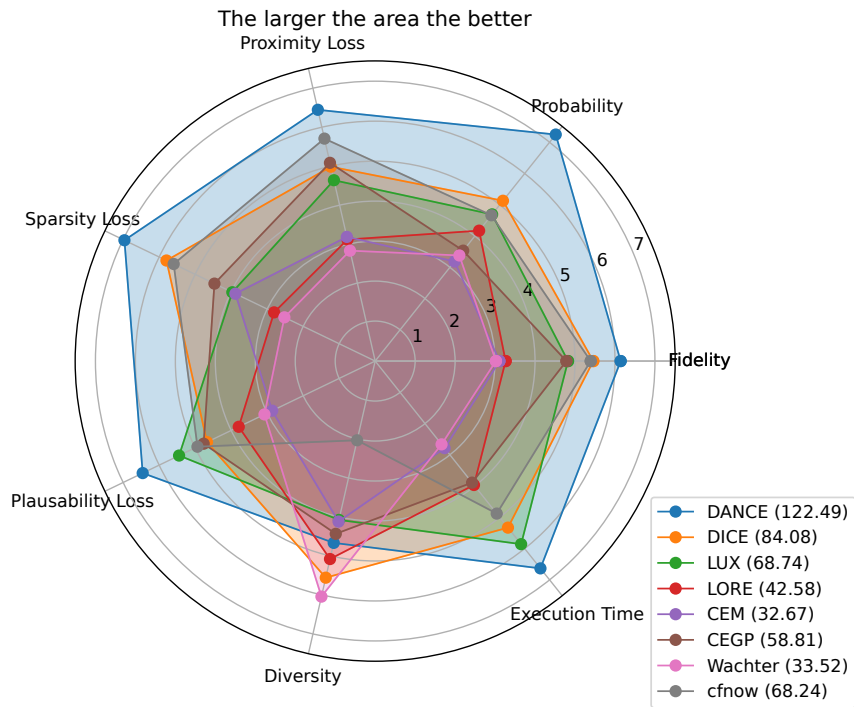


Figure 3: Combined evaluation metric visualized in a form of spiderplot. The larger the area, the better the method.

## 5.2 Ablation study

In this study, we removed the plausibility objective from the total loss function to observe how it affects the overall performance of other properties. In particular, we aimed at finding if plausibility negatively affects other metrics, especially such as diversity or sparsity. We tested these two models on the same set of datasets as discussed in previous section.

The difference in performance of the model with plausibility turned on relative to the model, where we turned off the plausibility component, is presented in Figure 4. The most noticeable difference is observed in plausibility, which is approximately 20% higher for the model incorporating the plausibility component. Conversely, the metrics visibly negatively impacted are diversity and sparsity. Also, the probability of the predictions of the black-box model for generated counterfactuals dropped by 10% in plausible model. The fidelity remains the same for both solutions with small changes to proximity and execution time.

The reduction in sparsity and diversity arises from the method’s inherently con-

strained search space for counterfactuals, guided by the relationship graph. This constraint leads to cascading modifications of dependent features within the graph, thereby reducing sparsity. Similarly, the diversity is constrained by the relationship graph, as there are areas of the feature space that cannot be explored without a negative impact on plausibility.

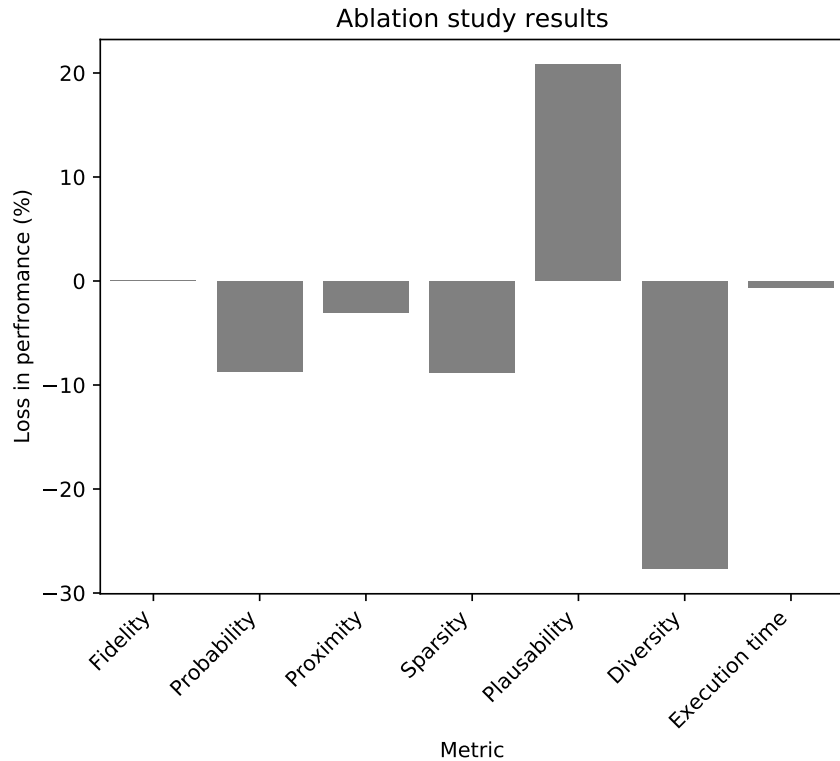


Figure 4: Decrease in performance with respect to different metrics of a model with plausibility optimization turned on.

## 6 Evaluation in the business case study

In this section we present a case study of the practical usage of DANCE method in real business case. The case study is a part of a SendGuard project carried out in collaboration with Freshmail company that one of the main operating goals is delivering tools that allow clients to design, manage, and send their own marketing campaigns through CPaaS approach to guard their quality. Despite adhering to best

practices and maintaining a strong emphasis on quality and consent, or due to the security challenges, the company mass distribution of emails frequently faces the risk of being misclassified as spam.

The core challenge driving this study stems from the observation that some clients of company’s CPaaS platform, despite developing ostensibly high-quality email campaigns (e.g., regularly updated subscriber lists, thematically relevant and appealing content), often achieve suboptimal user engagement rates. Analyzes revealed that issues such as poorly constructed subject lines or suboptimal sending times can overshadow otherwise robust campaign content. Consequently, these campaigns frequently yield results similar to, or even worse than, campaigns of objectively lower content quality (e.g., stale subscriber lists, purely promotional or repetitive messages).

In light of this, our primary objective was to devise a mechanism that suggests optimizations of selected campaign parameters, particularly those most visible to recipients (e.g., subject line elements, sending hour) and most likely to affect open and click rates. Rather than relying solely on heuristic guidelines, we sought a data-driven approach that would integrate expert knowledge about email marketing practices while respecting the intricate dependencies among features. In this case, the counterfactuals delivered by DANCE are a solution to our case. The overall idea of the system incorporating DANCE method is presented in Figure 5. In the following sections we elaborate on the dataset we used and results obtained with our approach.

## 6.1 Dataset description

In our study we used company’s own dataset spanning the period of 2019 to 2021. The total number of analyzed campaigns exceeded one million, though for model building we utilized a stratified sample of 100,000 campaigns (66% for training, 33% for testing). This sample captured a broad cross-section of sending behaviors, content styles, and thematic tags. Importantly, the dataset does not include any personal or sensitive information. By design, only the most influential high-level parameters were retained, thereby ensuring broad applicability across different types of email campaigns. This not only avoids potential biases or discrimination in feature selection but also makes the modeling approach scalable regardless of individual subscriber histories or sensitive demographic data. Each campaign record was described by the following primary features:

- Tag (e.g., Sport, Heavy-Industry, Events, Toys, etc.): Captures the general content category.
- Sending Hour and Day of the Week: Indicate the temporal configuration of

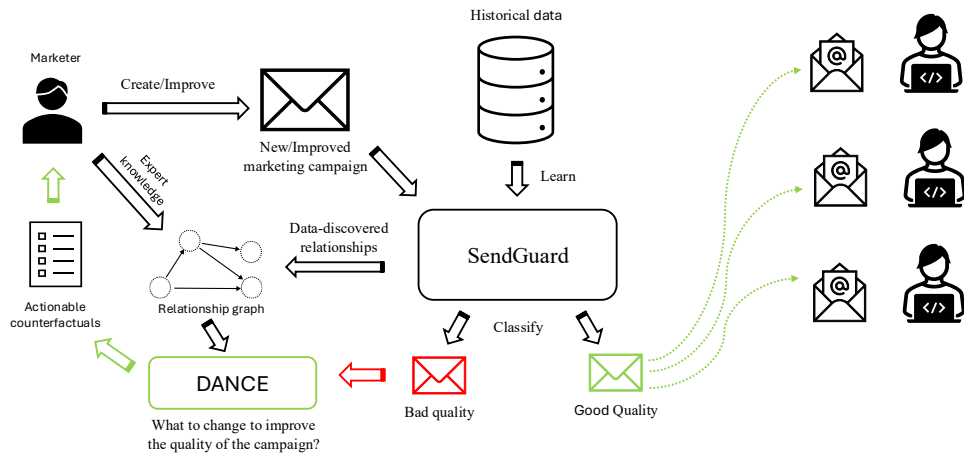


Figure 5: Workflow of the case study. The marketing campaign is processed through the SendGuard system to assess its quality. If the campaign is deemed of poor quality, the DANCE method generates counterfactual suggestions for potential modifications to enhance its possible open rate among addressees.

the campaign.

- **Content Composition:** Includes the number of links, the number of images, and a text-to-HTML ratio measure.
- **Subject Line Properties:** Subject length, presence of personalization tokens, emotive language, or question marks.

The target variable identified whether a campaign was considered *bad quality* (0) or *neutral/good quality* (1). These classes were derived from aggregate open rates, click rates, spam complaint rates, and unsubscribe rates, combined into a weighted score. This approach allowed us to separate lower-performing campaigns from those reaching acceptable or positive engagement benchmarks.

For the core predictive model, we employed the Explainable Boosting Machine (EBM) from the InterpretML toolkit achieving the following evaluation metrics: Accuracy: 0.6707, Recall: 0.6707, Precision: 0.6724, F1 Score: 0.6427, ROC AUC: 0.7471. Our primary aim was not to maximize predictive accuracy at all costs. Instead, we required a sufficiently robust classifier that could differentiate between suboptimal and acceptable campaigns while remaining interpretable. The ROC AUC of approximately 0.75 satisfied our baseline requirement for deployment and subsequent counterfactual analysis.

## 6.2 Relationship graph

A key premise of our method is that the optimal campaign parameters must reflect established best practices and domain-specific insights. For example, subject lines containing numbers (e.g., "5 Ways to...") or percentages (e.g., "Save 20%") often draw attention and bolster open rates. Conversely, overuse of emotional triggers or special symbols can trigger spam filters or frustrate recipients. Similarly, it is widely acknowledged that sending hours can significantly affect campaign performance, as recipients in certain industries are more likely to engage with emails during specific windows (e.g. early morning for B2B segments). Through close collaboration with marketing experts, we formalized these observations as a set of business rules governing how features such as `title_has_numbers`, `title_has_emotions`, `title_has_emojis`, and `campaign_sent_hour` should interplay. The business rules were then encoded in the relationship graph used by the DANCE method and are depicted in Figure 6. Notably, the brand context (B2B vs. B2C) and content category (tag) further modulate which strategies are likely to resonate with different audiences. This expert knowledge prevents the optimization process from suggesting unrealistic or domain-inconsistent changes—thereby ensuring the feasibility and credibility of any recommended modifications.

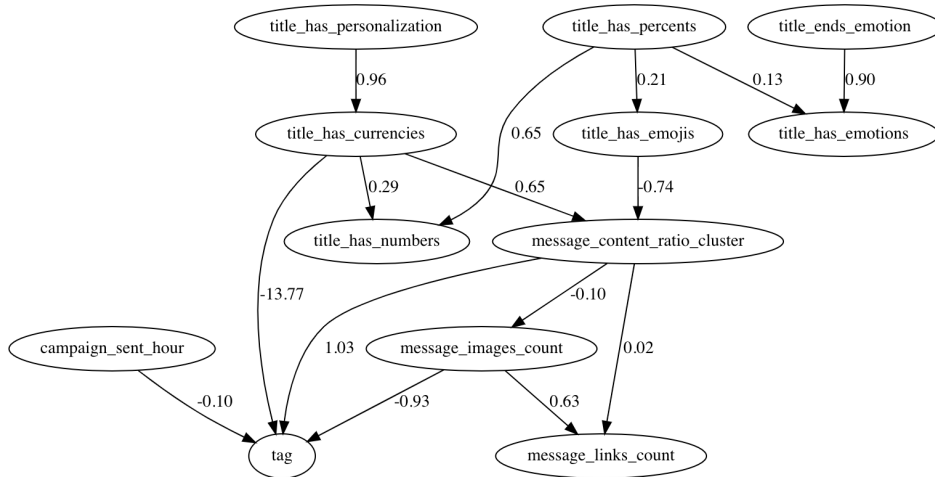


Figure 6: Relationship graph for the business case, created in collaboration in domain experts from the marketing field.

### 6.3 Counterfactual generation

To translate the above insights into actionable changes, we used DANCE that integrates both the learned model (EBM) and expert-driven constraints. This prevents suggestions that violate fundamental marketing principles or appear unrealistic in real-world deployments. In keeping with our initial design premise - to optimize only those parameters that recipients directly perceive before deciding whether to open a message or mark it as spam – we deliberately excluded from the set of optimizable features any that pertain explicitly to the content domain (tag) or to the overall message composition features. The rationale behind this constraint is twofold: first, thematic or domain-specific elements often require more substantial, brand-aligned revisions than simple parameter tweaks; second, altering deeper structural aspects of a campaign’s body (e.g., message layout, multimedia elements) goes beyond the minimal, high-impact changes that our mechanism aims to propose. In practice, the counterfactual generator identifies campaigns predicted to be *bad quality* (0) and proposes minimal yet meaningful feature shifts-such as modifying sending hour or introducing certain elements in the subject line-that could alter the model’s prediction to *neutral/good quality* (1). It does so by:

1. Checking feasible ranges and valid combinations for each allowable feature (e.g., limiting emotive punctuation in B2B contexts).
2. Prioritizing changes that are easiest to implement and most likely to improve engagement (e.g., adjusting `campaign_sent_hour` before attempting more drastic subject line modifications).
3. Maintaining a record of which features were changed and by how much, allowing marketers to evaluate both the acceptability and practical effort of each proposed adjustment.

### 6.4 Results and discussion

We tested our approach on a holdout set of 5,000 campaigns initially classified as *bad quality*. The counterfactual generator was able to propose at least one successful modification (i.e., one that changed the predicted class to *neutral/good quality*) for 3,248 samples, corresponding to 64.96% of this subset.

The sending hour (`campaign_sent_hour`) was by far the most common parameter to change (4,455 times), suggesting that a poorly timed send can markedly reduce engagement. The next most frequent changes involved the presence of emojis, numbers, and percentages in the subject line.

Additionally, 4,351 of the generated counterfactuals required exactly one feature change, while 732 involved two features. Only 107 cases required three or

more modifications. These findings confirm that even relatively small tweaks—especially in timing—can often suffice to transition a campaign from low-performing to adequate or better. The exemplary explanation of a sample campaign with domain expert comment regarding it was presented in Table 3.

In the illustrated example in Table 3, the DANCE mechanism proposed modifications to the subject line by removing percentages and emojis. This combination is commonly encountered in promotional campaigns within the "Cosmetics and Beauty" domain, where messages often highlight discounts or special offers. However, such content frequently receives a lukewarm reception and can even be perceived negatively. Consequently, the recommended adjustment encourages employing alternative content types rather than relying primarily on explicit promotional cues. Moreover, the mechanism advised changing the dispatch time from 11:00 AM to 8:00 AM. Empirical observations show that this audience segment is more inclined to engage with such content during morning inbox checks; messages sent later in the workday are frequently deprioritized and overlooked as lower-importance communications.

To further verify that domain constraints were respected, we grouped campaigns by tag (B2B, B2C, Mixed) and examined the statistical distribution of proposed feature values. Notably, the distribution of `campaign_sent_hour` in post-optimization campaigns varied significantly across these segments, as indicated by a chi-square test ( $\chi^2 = 104.45$ , and  $p < 0.000001$ ), suggesting the mechanism indeed adjusted sending times in ways consistent with the distinct preferences of different audience groups. This alignment with established industry practices underscores the value of incorporating domain expertise into the optimization logic, rather than relying on purely data-driven heuristics.

## 7 Summary

Our research presented in this paper addresses the limitations of existing counterfactual generation methods that often neglect the intricate dependencies between features, resulting in counterfactuals that are unrealistic, impractical, or misaligned with domain-specific requirements, such as industry standards, audience preferences, or brand guidelines. These shortcomings hinder their adoption in real-world applications.

To overcome these challenges, we propose a novel method called *Plausible Constrained Counterfactuals* that incorporates feature dependencies into the counterfactual generation process. The approach learns the structure and magnitude of these dependencies, expressed as linear or nonlinear constraints, either directly from the data or provided by domain experts. By enforcing these constraints, the

generated counterfactuals are plausible, actionable, and aligned with real-world requirements.

Our method optimizes a custom cost function that balances plausibility, diversity, and sparsity, using the Tree-structured Parzen Estimator algorithm to generate high-quality counterfactuals. Case studies demonstrate its effectiveness in delivering domain-relevant explanations that outperform existing methods on widely used evaluation metrics. This advancement highlights the potential of structured counterfactuals to enhance interpretability and utility in applications such as email marketing, where actionable insights are critical for refining strategies and improving engagement.

The motivation for our research is twofold. First, we introduced a practical business case study that allowed us for grounding our work on a real-life application for a start. It is worth noting, that the Freshmail Company that collaborated with us in the Sendguard project, deployed its results in practical security and marketing operations. However, the usefulness and applicability of our approach extends far beyond this domain, and was also evaluated on 140 open datasets from OpenML. The ability to generate plausible and actionable counterfactuals is crucial in many fields where understanding causality and ensuring practical feasibility are key to other applications. In healthcare, for example, counterfactuals can aid in personalized treatment plans by suggesting specific changes that could improve patient outcomes [26]. In industry, they can be used for predictive maintenance, helping identify conditions under which equipment failure could be avoided [8]. Other areas, such as finance, education, and policy-making, also stand to benefit from this methodology, where counterfactuals can guide decision-making and improve outcomes by considering realistic interventions in complex systems.

Ensuring the plausibility and adherence to domain knowledge when generating counterfactuals significantly enhances the practical value of this type of XAI methods. By grounding the suggestions in the specific constraints and nuances of each domain, the counterfactuals become not only more actionable but also more realistic and relevant. This ensures that the proposed interventions are not just theoretically possible but also feasible and effective in practice.

## **Acknowledgments**

This work was supported in part by the Project "SendGuard—Improving the Security of Recipients Innovative Tool Based on Machine Learning Technology and Artificial Intelligence to Fight with the Problem of Spam and Phishing in Marketing and Transactional E-Mail Messages" co-financed from the Funds of European Regional Development Fund under Project POIR.01.01.01-00-0202/19-02; The re-

search has been supported by a grant from the Priority Research Area (DigiWorld) under the Strategic Programme Excellence Initiative at Jagiellonian University.

## References

- [1] Adel Abusitta, Miles Q. Li, and Benjamin C.M. Fung. Survey on explainable ai: Techniques, challenges and open issues. *Expert Systems with Applications*, 255:124710, 2024.
- [2] Stefan Aeberhard and M. Forina. Wine. UCI Machine Learning Repository, 1992. DOI: <https://doi.org/10.24432/C5PC7J>.
- [3] Charu C. Aggarwal, Alexander Hinneburg, and Daniel A. Keim. On the surprising behavior of distance metrics in high dimensional space. In Jan Van den Bussche and Victor Vianu, editors, *Database Theory — ICDT 2001*, pages 420–434, Berlin, Heidelberg, 2001. Springer Berlin Heidelberg.
- [4] Hubert Baniecki and Przemyslaw Biecek. Adversarial attacks and defenses in explainable artificial intelligence: A survey. *Information Fusion*, 107:102303, 2024.
- [5] Bernd Bischl, Giuseppe Casalicchio, Taniya Das, Matthias Feurer, Sebastian Fischer, Pieter Gijsbers, Subhaditya Mukherjee, Andreas C Müller, László Németh, Luis Oala, Lennart Purucker, Sahithya Ravi, Jan N van Rijn, Prabhant Singh, Joaquin Vanschoren, Jos van der Velde, and Marcel Wever. Openml: Insights from 10 years and more than a thousand papers. *Patterns*, 6(7):101317, 2025.
- [6] Szymon Bobek, Paloma Korycińska, Monika Krakowska, Maciej Mozolewski, Dorota Rak, Magdalena Zych, Magdalena Wójcik, and Grzegorz J. Nalepa. User-centric evaluation of explainability of ai with and for humans: A comprehensive empirical study. *International Journal of Human-Computer Studies*, 205:103625, 2025.
- [7] Szymon Bobek and Grzegorz J. Nalepa. Local universal rule-based explainer (lux), 2025.
- [8] Szymon Bobek and Grzegorz J. Nalepa. Tsproto: Fusing deep feature extraction with interpretable glass-box surrogate model for explainable time-series classification. *Information Fusion*, page 103357, 2025.

- [9] Raphaela Butz, Renée Schulz, Arjen Hommersom, and Marko van Eekelen. Investigating the understandability of xai methods for enhanced user experience: When bayesian network users became detectives. *Artificial Intelligence in Medicine*, 134:102438, 2022.
- [10] Chaofan Chen, Oscar Li, Chaofan Tao, Alina Jade Barnett, Jonathan Su, and Cynthia Rudin. This looks like that: deep learning for interpretable image recognition. In *Proceedings of the 33rd International Conference on Neural Information Processing Systems*, Red Hook, NY, USA, 2019. Curran Associates Inc.
- [11] Yu-Liang Chou, Catarina Moreira, Peter Bruza, Chun Ouyang, and Joaquim Jorge. Counterfactuals and causability in explainable artificial intelligence: Theory, algorithms, and applications. *Information Fusion*, 81:59–83, 2022.
- [12] DARPA. Explainable Artificial Intelligence.
- [13] Raphael Mazzine Barbosa de Oliveira, Kenneth Sörensen, and David Martens. A model-agnostic and data-independent tabu search algorithm to generate counterfactuals for tabular, image, and text data. *European Journal of Operational Research*, 2023.
- [14] Amit Dhurandhar, Tejaswini Pedapati, Avinash Balakrishnan, Pin-Yu Chen, Karthikeyan Shanmugam, and Ruchir Puri. Model agnostic contrastive explanations for structured data, 2019.
- [15] EU. Proposal for a Regulation of the European Parliament and of the Council Laying Down Harmonised Rules on Artificial Intelligence (Artificial Intelligence Act) and Amending Certain Union Legislative Acts, 2021.
- [16] Wojciech Gałka, Jan G. Bazan, Urszula Bentkowska, Kamil Szwed, Marcin Mrukowicz, Paweł Drygaś, Lech Zaręba, Marcin Szpyrka, Piotr Suszalski, and Sebastian Obara. Aggregation-based ensemble classifier versus neural networks models for recognizing phishing attacks. *IEEE Access*, 13:48469–48487, 2025.
- [17] Riccardo Guidotti. Counterfactual explanations and how to find them: literature review and benchmarking.
- [18] Riccardo Guidotti, Anna Monreale, Fosca Giannotti, Dino Pedreschi, Salvatore Ruggieri, and Franco Turini. Factual and counterfactual explanations for black box decision making. *IEEE Intelligent Systems*, 34(6):14–23, 2019.

- [19] Kentaro Kanamori, Takuya Takagi, Ken Kobayashi, and Hiroki Arimura. Dace: Distribution-aware counterfactual explanation by mixed-integer linear optimization. In Christian Bessiere, editor, *Proceedings of the Twenty-Ninth International Joint Conference on Artificial Intelligence, IJCAI-20*, pages 2855–2862. International Joint Conferences on Artificial Intelligence Organization, 7 2020. Main track.
- [20] Amir-Hossein Karimi, Gilles Barthe, Borja Balle, and Isabel Valera. Model-agnostic counterfactual explanations for consequential decisions. In Silvia Chiappa and Roberto Calandra, editors, *The 23rd International Conference on Artificial Intelligence and Statistics, AISTATS 2020, 26-28 August 2020, Online [Palermo, Sicily, Italy]*, volume 108 of *Proceedings of Machine Learning Research*, pages 895–905. PMLR, 2020.
- [21] Been Kim, Rajiv Khanna, and Oluwasanmi Koyejo. Examples are not enough, learn to criticize! criticism for interpretability. In *Proceedings of the 30th International Conference on Neural Information Processing Systems, NIPS’16*, page 2288–2296, Red Hook, NY, USA, 2016. Curran Associates Inc.
- [22] Yin Lou, Rich Caruana, Johannes Gehrke, and Giles Hooker. Accurate intelligible models with pairwise interactions. In *Proceedings of the 19th ACM SIGKDD International Conference on Knowledge Discovery and Data Mining, KDD ’13*, page 623–631, New York, NY, USA, 2013. Association for Computing Machinery.
- [23] Divyat Mahajan, Chenhao Tan, and Amit Sharma. Preserving causal constraints in counterfactual explanations for machine learning classifiers, 2020.
- [24] Tim Miller. Explanation in artificial intelligence: Insights from the social sciences. *Artificial Intelligence*, 267:1–38, 2019.
- [25] Ramaravind K. Mothilal, Amit Sharma, and Chenhao Tan. Explaining machine learning classifiers through diverse counterfactual explanations. In *Proceedings of the 2020 Conference on Fairness, Accountability, and Transparency, FAT\* ’20*, page 607–617, New York, NY, USA, 2020. Association for Computing Machinery.
- [26] Maciej Mozolewski, Betül Bayrak, Kerstin Bach, and Grzegorz J. Nalepa. From prototypes to sparse ecg explanations: Shap-driven counterfactuals for multivariate time-series multi-class classification, 2025.

- [27] Axel Parmentier and Thibaut Vidal. Optimal counterfactual explanations in tree ensembles. In Marina Meila and Tong Zhang, editors, *Proceedings of the 38th International Conference on Machine Learning*, volume 139 of *Proceedings of Machine Learning Research*, pages 8422–8431. PMLR, 18–24 Jul 2021.
- [28] Chris Russell. Efficient search for diverse coherent explanations. In *Proceedings of the Conference on Fairness, Accountability, and Transparency*, FAT\* '19, page 20–28, New York, NY, USA, 2019. Association for Computing Machinery.
- [29] Stuart Russell. *Artificial Intelligence and the Problem of Control*, pages 19–24. Springer International Publishing, Cham, 2022.
- [30] Shohei Shimizu, Patrik O. Hoyer, Aapo Hyvärinen, and Antti Kerminen. A linear non-gaussian acyclic model for causal discovery. *J. Mach. Learn. Res.*, 7:2003–2030, December 2006.
- [31] Jasper van der Waa, Elisabeth Nieuwburg, Anita Cremers, and Mark Neerinx. Evaluating xai: A comparison of rule-based and example-based explanations. *Artificial Intelligence*, 291:103404, 2021.
- [32] Arnaud Van Looveren and Janis Klaise. Interpretable counterfactual explanations guided by prototypes. In Nuria Oliver, Fernando Pérez-Cruz, Stefan Kramer, Jesse Read, and Jose A. Lozano, editors, *Machine Learning and Knowledge Discovery in Databases. Research Track*, pages 650–665, Cham, 2021. Springer International Publishing.
- [33] Sandra Wachter, Brent D. Mittelstadt, and Chris Russell. Counterfactual explanations without opening the black box: Automated decisions and the GDPR. *CoRR*, abs/1711.00399, 2017.
- [34] Shuhei Watanabe. Tree-structured parzen estimator: Understanding its algorithm components and their roles for better empirical performance, 2023.
- [35] Patryk Wielopolski, Oleksii Furman, Jerzy Stefanowski, and Maciej Zięba. Probabilistically plausible counterfactual explanations with normalizing flows, 2024.
- [36] Yunxia Zhao. Fast real-time counterfactual explanations, 2020.
- [37] Xun Zheng, Bryon Aragam, Pradeep Ravikumar, and Eric P. Xing. Dags with no tears: continuous optimization for structure learning. In *Proceedings of the*

## A Statistical tests for quantitative evaluation

With 8 algorithms and 140 datasets, we had  $7 \times 973$  degrees of freedom, respectively. This enabled us to establish that the critical distance for the post-hoc Nemenyi test, with  $F(7, 973)$  and  $\alpha = 0.05$  is 0.75 for all the subsequent cases.

In Figure 7 the performance of DANCE method was presented in comparison to other approaches in terms of plausibility defined in Equation (4). It obtained highest scores and the difference is statistically significant. There were datasets where DANCE achieved worse results in comparison to LUX, however, this is caused by the fact that LUX is endogenous explainer, hence it produces explanations that are selected from the existent dataset, hence always plausible.

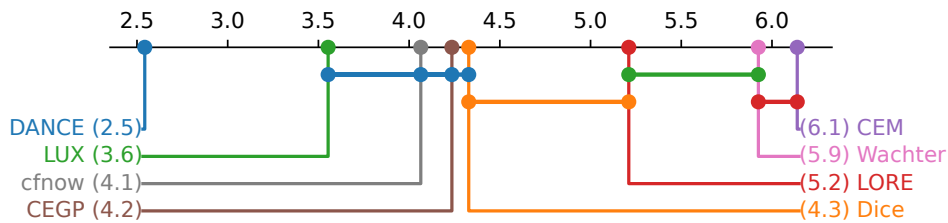


Figure 7: Critical distance plot for plausibility loss.

Figure 8 presents the results DANCE achieved in terms of diversity metric defined in Equation (7). It is notable that the results were comparable to LORE and CEGP, but is statistically worse than Dice and Wachter. It can be observed that the diversity comes with a trade off to plausibility, by comparing Figure 8 and Figure 7. This is especially visible in case of Wachter, which took opposite places for both of these metrics. In many cases assuring plausibility comes at a cost of diversity, especially where there are strong relationships between variables, that prevent diverse changes to their values.

Figure 9 shows the results of the proximity evaluation defined in Equation (5). The DANCE obtained the best results along with cfnow. This metric is related to the sparsity loss presented in Figure 10 and defined in Equation (6). Methods that obtained high sparsity were generally able to achieve high proximity.

Figure 11 presents the results for the fidelity metric that is sometimes also referred to as correctness. It measures ratio of correctly discovered counterfactuals

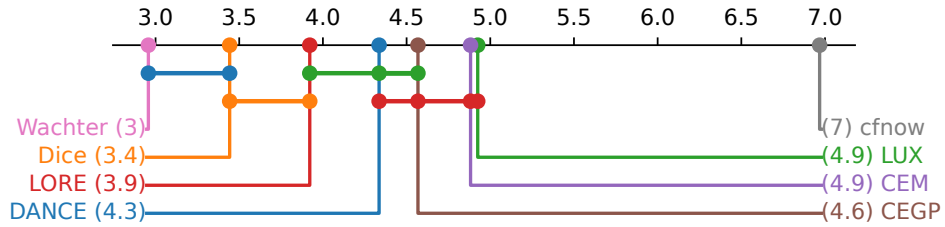


Figure 8: Critical distance plot for diversity.

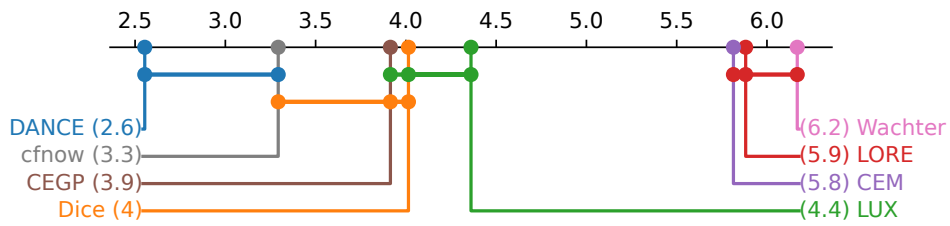


Figure 9: Critical distance plot for proximity loss.

(counterfactuals that indeed changed the prediction of the model). A clearly visible two clusters of methods were formed here with a significant gap between them.

Figure 12 shows the results obtained for the probability metric. It is highly correlated with fidelity, as it shows the probability of the counterfactual obtained from the balckbox model for a desired class. However, in this plot it can be seen that although the fidelity metric was similar to several algorithms, in case of probability metric, the DANCE stands out as the best one.

The evaluation of execution time was presented in Figure 13. It is worth noting that only the execution time of the search for counterfactuals were measures in the case of DANCE. The creation of a relationship graph was not included in the

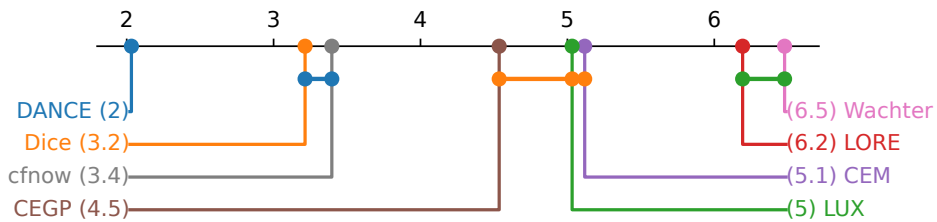


Figure 10: Critical distance plot for sparsity loss.

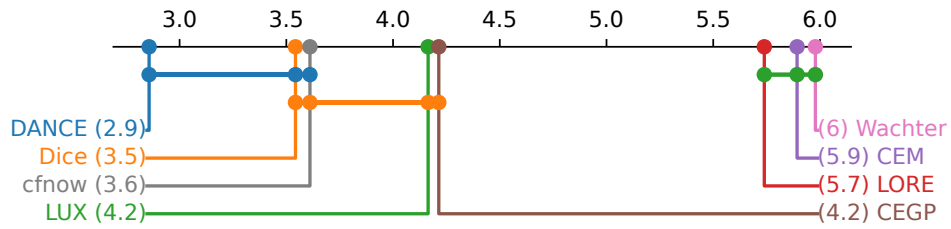


Figure 11: Critical distance plot for fidelity.

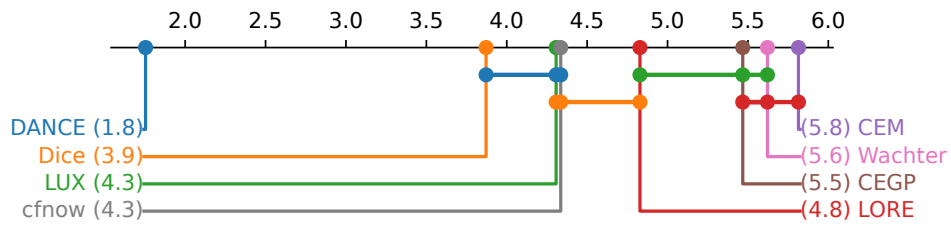


Figure 12: Critical distance plot for probability.

measurements. The creation of a relationship graph is very time consuming, but it is a one-time procedure that can be combined with balck-box model training, hence we excluded it from the evaluation.

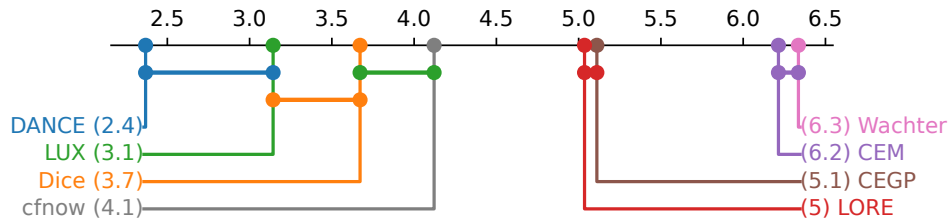


Figure 13: Critical distance plot for execution time.

Table 1: Comparison of Counterfactual Explanation Methods. There is no method that addresses all of the properties defined in columns.

Method	Optimization Mechanism	Diversity	Sparsity	Proximity	Plausibility	Model-Agnosticism	Expert-Based Constraints
DICE [25]	Various	Yes	Yes	Yes	Constraint-based	Yes	Range-based
DCE [28]	Linear programming	Yes	Yes	Yes	Minimal	Linear models only	No
CEM [14]	FISTA optimizer	No	No	Yes	Autoencoder-based	Yes	Range-based
EBCF [23]	Gradient-based	No	No	Yes	Autoencoder + manually encoded causal constraints	Yes	Yes
DACE [19]	CPLEX optimizer	No	No	Yes	Density-based / outlier-based	Linear and tree-based	No
MACE [20]	SAT solvers	Yes	Yes	Yes	Constraint-based	No	Range-based
OCEAN [27]	Custom loss function	Not naturally	No	Yes	Density-based / outlier-based	Only for tree ensembles	Logical and Linear
CEGP [32]	FISTA + K-D Tree search	No	Yes	Yes	Autoencoder-based	Yes	No
PPCF [35]	Gradient-based	No	No	Yes	Density-based	Requires gradients	No
LUX [7]	Entropy and distance	Not naturally	No	Yes	Density-based	Yes	No
LORE [18]	Entropy and distance	No	No	Yes	Density-based	Yes	No
Wachter [33]	Simplex	No	Yes	Yes	No	Yes	No
CFNOW [13]	Tabu search	No	Yes	Yes	No	Yes	No

Table 2: Summary of results from quantitative evaluation. The value represent average rank of the method over 140 datasets. The lower the better. The  $\uparrow$  denotes winners that were statistically significantly better the the rest.

	DANCE	Dice	LUX	LORE	CEM	CEGP	Wachter	cfnow
Fidelity	<b>2.86</b>	3.54	4.16	5.74	5.89	4.21	5.98	3.61
Probability	<b>1.75</b> $\uparrow$	3.87	4.31	4.83	5.81	5.47	5.62	4.34
Proximity Loss	<b>2.55</b>	4.01	4.36	5.88	5.81	3.91	6.17	3.29
Sparsity Loss	<b>2.03</b> $\uparrow$	3.21	5.03	6.19	5.12	4.54	6.48	3.40
Plausability Loss	<b>2.54</b> $\uparrow$	4.33	3.55	5.21	6.14	4.24	5.92	4.06
Diversity	4.34	3.44	4.92	3.92	4.88	4.57	<b>2.96</b>	6.97
Execution Time	<b>2.37</b>	3.67	3.14	5.04	6.21	5.11	6.34	4.12
Total Wins	<b>6</b>	0	0	0	0	0	1	0

Table 3: Comparison of feature values between sample campaign marked as *bad quality* and counterfactual generated with DANCE. Bold rows indicate values that were changed by the mechanism.

Campaign feature	Origin	DANCE
title_has_numbers	1	1
title_has_personalization	0	0
<b>title_has_percents</b>	<b>1</b>	<b>0</b>
title_has_emotions	1	1
title_has_questions	0	0
title_has_quotes	0	0
<b>title_has_emojis</b>	<b>1</b>	<b>0</b>
title_has_currencies	0	0
title_has_brackets	0	0
title_ends_question	0	0
title_ends_emotion	1	1
<b>campaign_sent_hour</b>	<b>11</b>	<b>8</b>
campaign_sent_dayofweek	5	5
campaign_sent_day	28	28
tag	Cosmetic, Beauty	Cosmetic, Beauty
message_content_ratio_cluster	1	1
message_links_count	24.0	24.0
message_images_count	14.0	14.0